

1.9. OPTICAL POTENTIAL AND TRANSFER

87

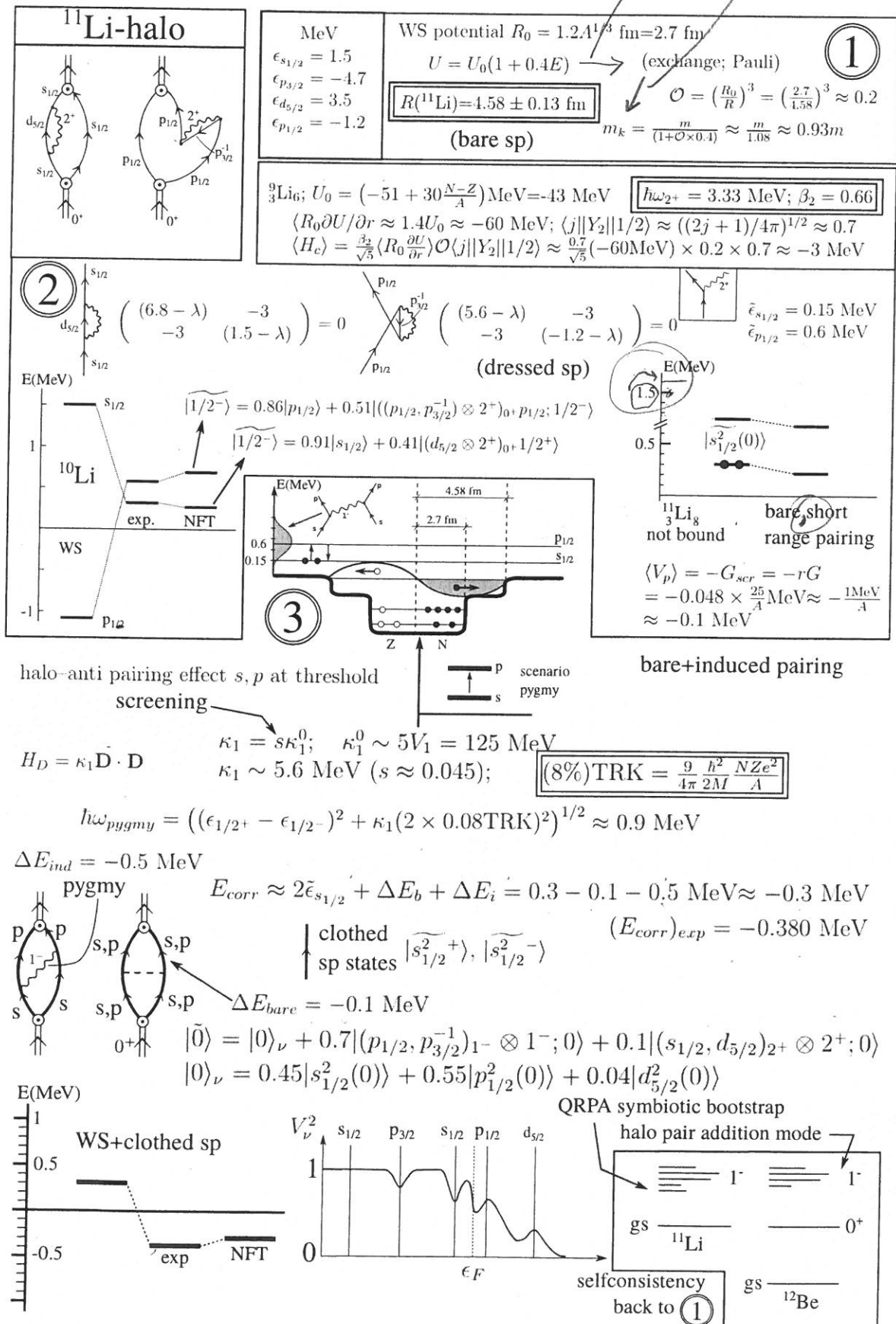


Figure 1.9.1

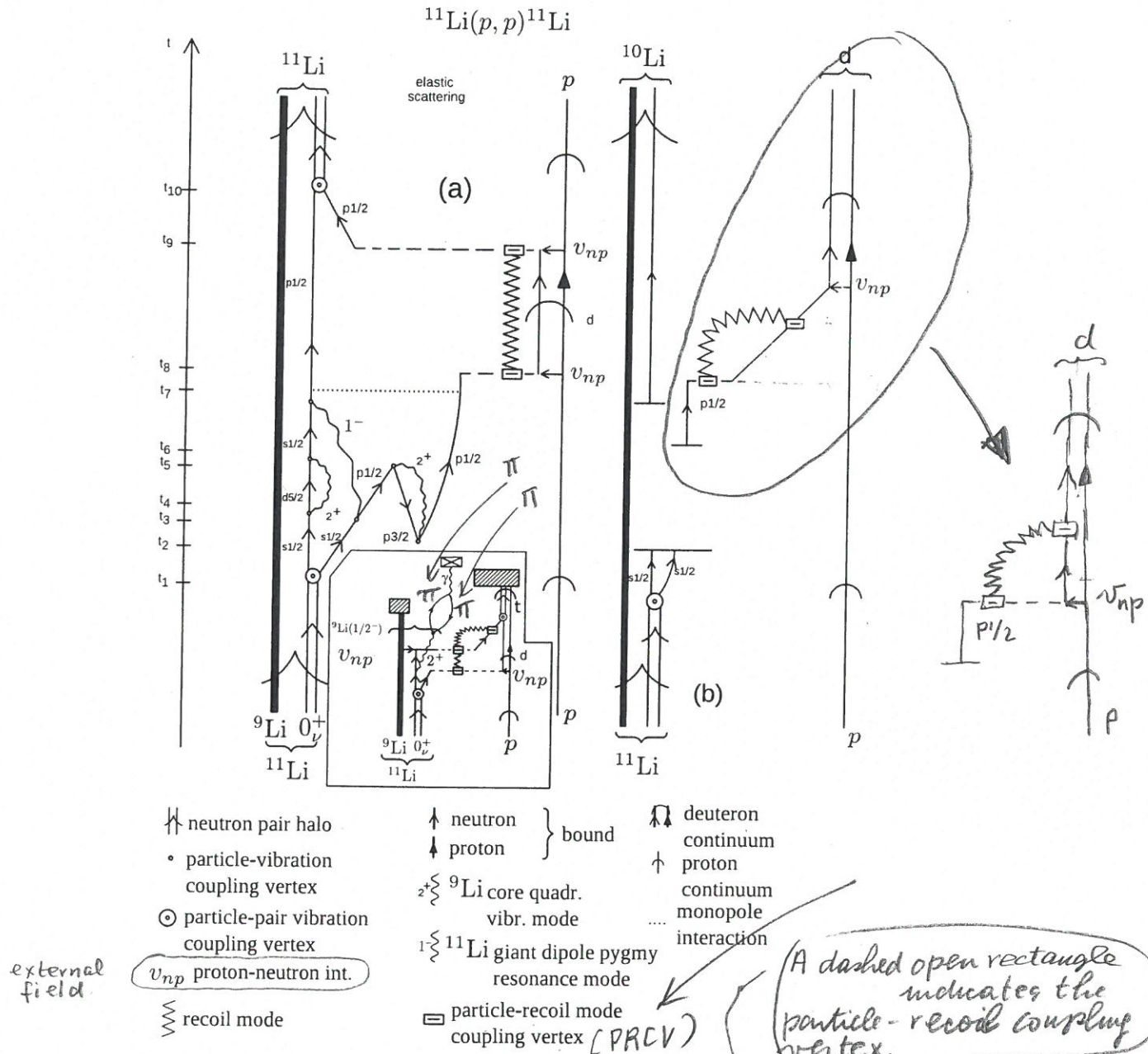
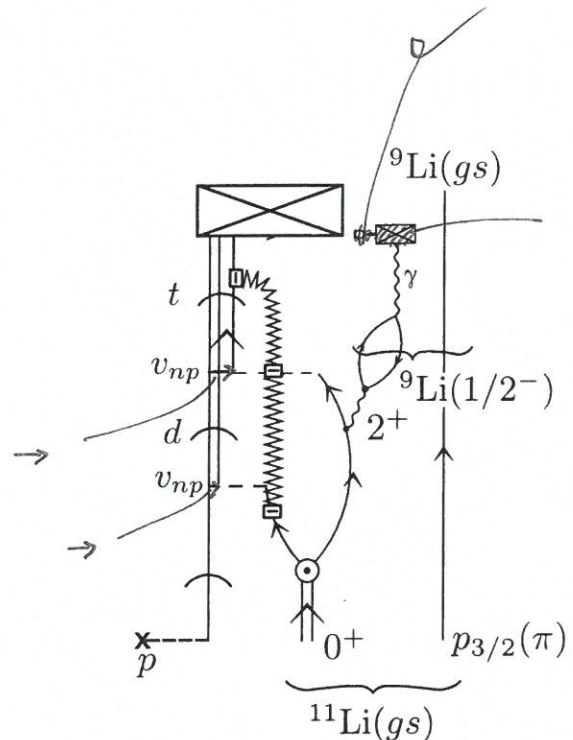


Figure 1.9.2: (a) NFT-diagram describing one of the processes contributing to the elastic reaction $^{11}\text{Li}(p, p)^{11}\text{Li}$ as the system propagates in time (polarization contribution to the global (mean field) optical potential). In the inset, a schematic NFT diagram describing the process $^{11}\text{Li}(p, t)^{9}\text{Li}(1/2^-)$ is displayed. A crossed box represents a γ -detector, while hatched rectangles particle detectors. (b) Same as in (a) up to time t_8 (reason for which no details are repeated between t_2 and t_8). From there on the deuteron continues to propagate to the detector (together with the recoil mode). Likely, the neutron in ^{10}Li will break up before this event. Summing up, in the center of mass reference frame both p and ^{11}Li display asymptotic states in entrance as well as in exit channels in case (a), and only in the entrance channel in case (b), while in the exit channel only ^{10}Li ($^{9}\text{Li} + n$) and the deuteron do so.

it is the

that



Variety of pv-coupling vertices
(NFT)

○ pair
● surface
■ recoil

Figure 1.9.5: Gedanken γ -ray coincidence experiment $^1\text{H}(^{11}\text{Li}, ^9\text{Li})^3\text{H}$ and $^9\text{Li}(\text{gs}) + \gamma(E2; 2.69 \text{ MeV})$. In this case, the virtual quadrupole phonon associated with self-energy and vertex correction processes becomes real through the action of the (p, t) external field. Thus, it is not only that recoil modes are “measured” by detectors in connection with outgoing particles which have asymptotic wavefunctions, but also the quadrupole vibration, whose eventual γ -decay can be measured by the γ -detector.

(see Fig. 6.6.2 (II))

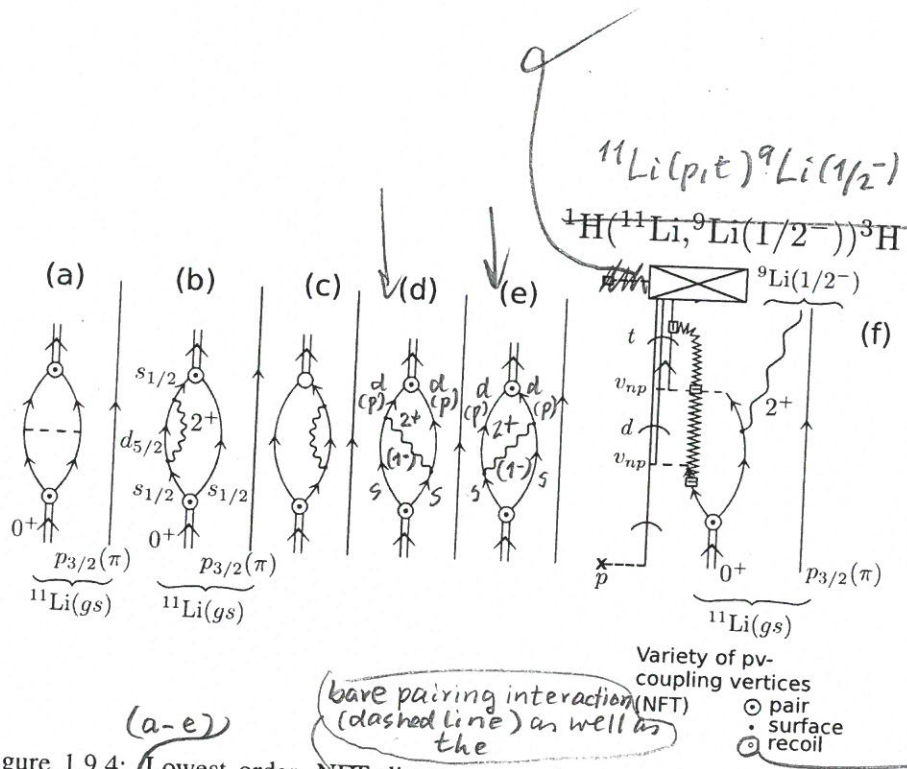


Figure 1.9.4: Lowest order, NFT diagrams associated with the processes contributing to the binding of the neutron halo Cooper pair (double arrowed line) of ^{11}Li to the core ^9Li through the exchange of the core quadrupole phonon (wavy line). Single arrowed lines describe the nucleon independent-particle motion of neutrons ($s_{1/2}$, $d_{5/2}$, etc.) as well as of protons ($p_{3/2}(\pi)$). (a) Bare interaction, four-point vertex (horizontal dashed line); (b, c) self energy, effective mass process dressing the $s_{1/2}(v)$ single-particle state; (d, e) vertex correction (induced interaction) renormalizing the vertex with which the pair addition mode couples to the fermion (dotted open circle); (f) NFT diagrams describing the inverse kinematics reaction $^{11}\text{H}(\text{Li}, ^9\text{Li}(1/2^-, 2.69 \text{ MeV}))^3\text{H}$ populating the first excited state of ^9Li . The jagged line represents the recoil mode carrying asymptotically to the detector the effect of the momentum mismatch associated with the transfer process (recoil). In this case of successive transfer, one for each transferred neutron ($^{11}\text{Li(gs)} + p \rightarrow ^{10}\text{Li} + d \rightarrow ^9\text{Li}(1/2^+) + t$). See also Sect. 2.6 as well as Sect. 6.1.

(similar diagram, but corresponding to correlation (CO) processes (see Fig. 4.2.4) dressing the $p_{1/2}$ state are not shown, see Figs. 1.9.2 and 1.9.3)

(the dashed horizontal line starting with a cross standing for the (p,t) probe)

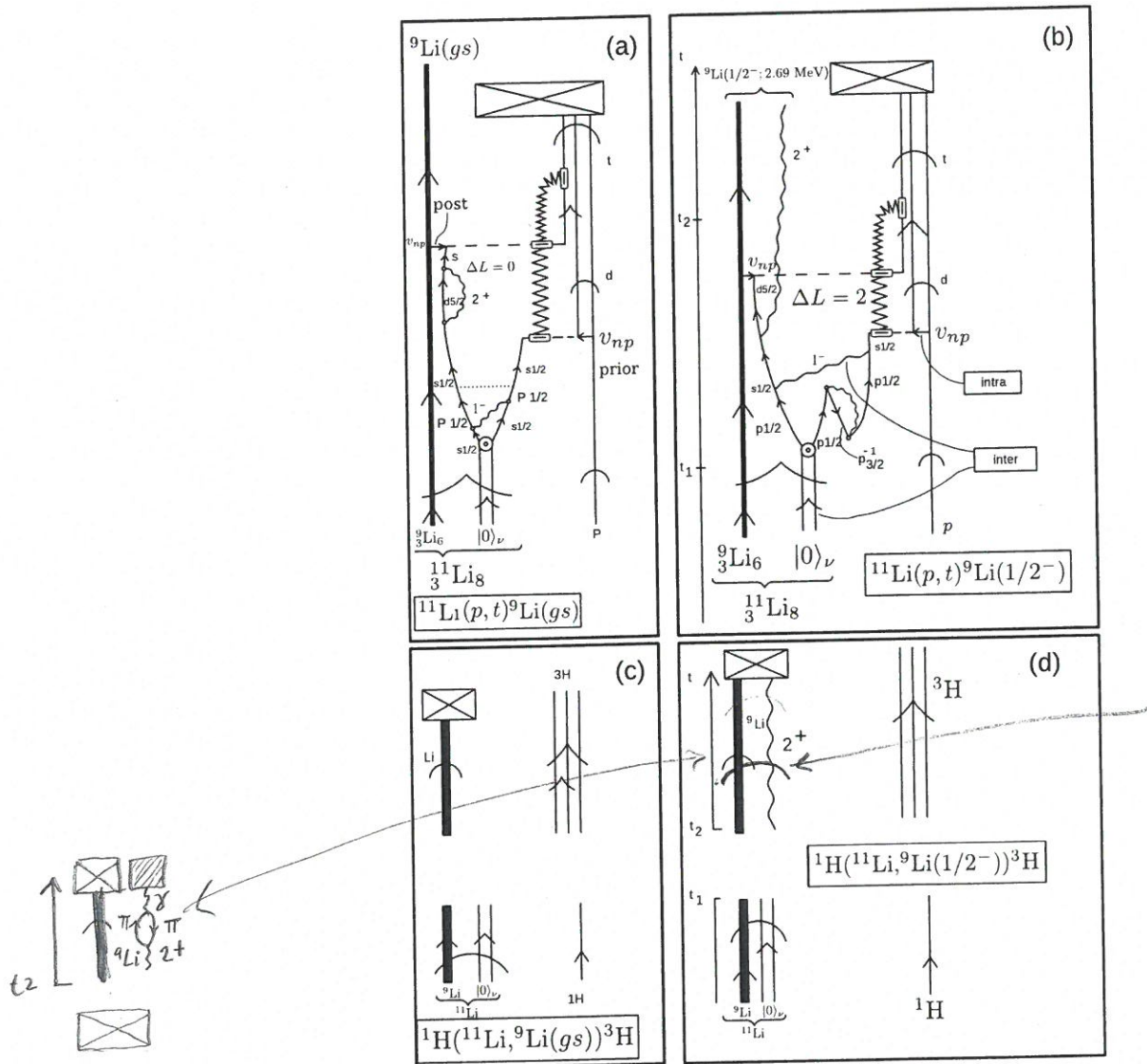


Figure 1.9.3: NFT representation of the reactions (a) $^{11}\text{Li}(p,t)^9\text{Li}(\text{gs})$, (b) $^{11}\text{Li}(p,t)^9\text{Li}(1/2^-)$, (c) $^1\text{H}(^{11}\text{Li},^9\text{Li}(\text{gs}))^3\text{H}$ and (d) $^1\text{H}(^{11}\text{Li},^9\text{Li}(1/2^-))^3\text{H}$. Time is assumed to run upwards. A single arrowed line represents a fermion (proton) (p) or neutron (n). A double arrowed line two correlated nucleons. In the present case two correlated (halo) neutrons (halo-neutron pair addition mode $|0>_v$). A heavy arrowed line represents the core system $^9\text{Li}(\text{gs})$. A standard pointed arrow refers to structure, while "round" arrows refer to reaction. A wavy line represents (particle-hole) collective vibrations, like the low-lying quadrupole mode of ^9Li , or the (more involved) dipole pygmy resonant state which, together with the bare pairing interaction (horizontal dotted line) binds the neutron halo Cooper pair to the core. A short horizontal arrow labels the proton-neutron interaction v_{np} responsible for the single-particle transfer processes, represented by an horizontal dashed line. A dashed open square indicates the particle-recoil coupling vertex. The jagged line represents the recoil normal mode resulting from the mismatch between the relative centre of mass coordinates associated with the mass partitions $^{11}\text{Li}+p$, $^{10}\text{Li}+d$ (virtual) and $^9\text{Li}+t$. The γ -detector and particle detectors are represented by a crossed rectangle. For further details see caption Fig. 1.9.2. (see Fig. 6.6.2)

| | $ \alpha\rangle$ | $ \beta\rangle$ | | $ \alpha\rangle$ | $ \beta\rangle$ | | $ \alpha\rangle$ | $ \beta\rangle$ |
|------------------|------------------|-----------------|--|------------------|-----------------|--------|------------------|-----------------|
| $ \alpha\rangle$ | -0.010 | -0.168 | | $ \alpha\rangle$ | -0.012 | -0.434 | $ \alpha\rangle$ | -0.011 |
| $ \beta\rangle$ | | 0.009 | | $ \beta\rangle$ | | 0.070 | $ \beta\rangle$ | 0.03 |

Table 1.C.1: Normalization matrices (see Eq. (1.7.73)) associated with the two $3/2^+$ states of ^{209}Bi , $|I\rangle$ and $|II\rangle$ (Fig. 1.7.11 (e)) (Bortignon, P. F. et al. (1977), table 4.6).

| | | Fig. 1.7.10 | | |
|-----|------|-------------|--------|---------|
| m | m' | (b) | (c) | (b)+(c) |
| I | II | 0.013 | -0.181 | -0.168 |
| II | II | 0.016 | -0.450 | -0.434 |
| I | II | 0.014 | -0.285 | -0.271 |

Table 1.C.2: Contributions to the off diagonal elements of the overlap matrix $M_{ii'}^{mm'}$ associated with the $3/2$ states in the basis $|\alpha\rangle, |\beta\rangle$ (Table 1.C.1). See also figure 4.1 of Bortignon, P. F. et al. (1977).

systematic mathematical procedure to deal with the spurious state (in this case due to the overcompleteness of the basis $\{|\alpha\rangle, |\beta\rangle\}$) one can also relate, within the framework of shell model calculations (see Eq. (1.C.1)), the asymmetry between $R(t, \alpha)$ and $R(\alpha, \alpha')$ to the finite overlaps between states $|\alpha\rangle$ and $|\beta\rangle$, as discussed in Sect. 1.5.

1.C.3 NFT (r+s) see pp. (109)_a and (109)_b

Appendix 1.D NFT and reactions

Nuclear Field Theory was systematically developed to describe nuclear structure processes. This fact did not prevent the translation into this graphical language of expressions which embodied the transition amplitude of a variety of reaction processes, in particular second order (in v_{np}) transition amplitudes associated with two nucleon transfer reactions¹³⁷.

The new feature to be considered regarding transfer processes and not encountered neither in structure, nor in elastic or anelastic processes, is the graphical representation of recoil effects. That is, a physical phenomenon associated with the change in the coordinate of relative motion reflecting the difference in mass partition between entrance (intermediate, if present) and exit channels. In fact, nuclear structure processes, do not affect the center of mass, with a proviso. In fact, the shell model potential violates the translational of the total nuclear Hamiltonian and, thus, single-particle excitations can be produced by a field proportional to the total center-of-mass coordinate. The translational invariance can be restored by including the effects of the collective field generated by a small displacement α of the nucleus. Such a displacement, in the x -direction, gives rise to a coupling which

¹³⁷Broglia (1975).

1.C.3 NFT($r+s$) ; linear theory

(109)
a

NFT is linear in the variety of particle-vibration coupling vertices. This is also valid concerning its extension to describe reaction processes, as can be seen from graph (a) of Fig. 1.C.2. For simplicity, this diagram and similar ones are drawn as displayed in Fig. 1.C.2 (b) (see also Fig. 1.1.3). However, in all cases the effects of recoil are properly taken into account following (a), as shown in e.g. Fig. 3.1.2 as well as in Section 5.1 within the framework of the DWBA, and in App. 5.C (Eqs. (5.C.6) and (5.C.7)) in the semiclassical approximation.

(109) b

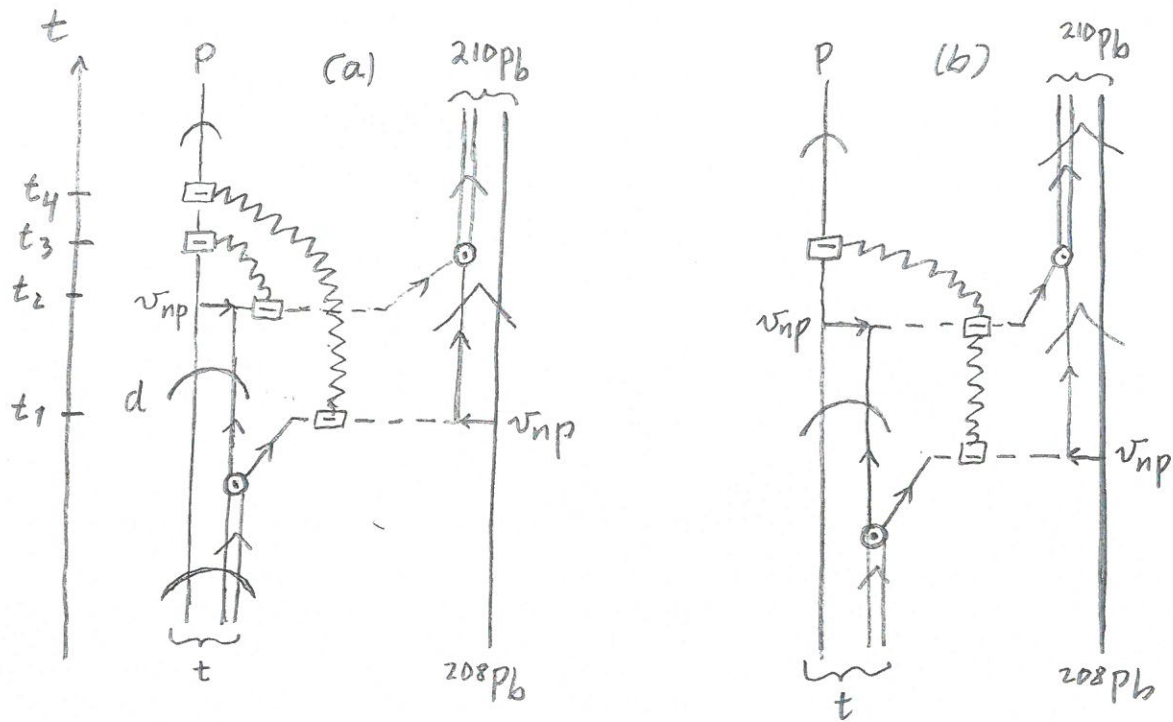


Fig. 1.C.2

NFT($r+s$) diagram describing the reaction $^{208}\text{Pb}(t, p) ^{210}\text{Pb}(gs)$ reaction. That is the population of the lowest energy, monopole spin additive mode of ^{208}Pb ~~over magnetized~~. Concerning the different symbols used, we refer to Figs. 1.1.3 and 1. In particular concerning the recoil mode (gagged lines) and the associated particle-recoil mode coupling vertex (dashed open rectangle) shown in (a). Also, of all the possible contributions associated with the ^{different} sequence of the process taking place in this graph at t_1, t_2, t_3 and t_4 (not shown), with the final outcome that the outgoing particle carries information to the detector of a transfer of **two neutron masses**. With this proviso in mind is that one can replace diagram (a) by diagram(b), (and only for simplicity).

CH₂

nucleon transfer reactions, the quantity (order parameter α'_0) which expresses the collectivity of the members of a pairing rotational band, reflects the properties of a coherent state ($|BCS\rangle$). In other words, it results from the sum over many contributions ($\sqrt{j_\nu + 1/2} U'_\nu V'_\nu$, see Sect. 2.4, also Sect. 6.4.3) all of them having the same phase. Consequently, the relative error decreases as the square root of the number contributions ($\approx N(0)\Delta \approx 4 \text{ MeV}^{-1} \times 1.4 \text{ MeV} \approx 6$ in the case of the superfluid nucleus ^{120}Sn).

There is a further reason which confers $\alpha'_0 = \sum_j (j + 1/2) U'_j V'_j$ a privileged position with respect to the single contributions $(j + 1/2) U'_j V'_j$. It is the fact that $\alpha'_0 = e^{2i\varphi} \sum_j (j + 1/2) U_j V_j = e^{2i\varphi} \alpha_0$ defines a privileged orientation in gauge space, α_0 being the order parameter referred to the laboratory system which makes an angle φ in gauge space with respect to the intrinsic system to which α'_0 is referred²³. In other words, the quantities α'_0 which measure the deformation of the superfluid nuclear system in gauge space, and the rotational frequency $\lambda = \hbar\dot{\varphi}$ in this space, and associated Coriolis force $-\lambda N_0$ felt by the nucleons referred to the body fixed frame, are the result of solving selfconsistently the BCS number²⁴.

gap equations $N_0 = \sum_j (2j + 1) \frac{1 - \frac{(\epsilon_j - \lambda)/\Delta}{\sqrt{1 + (\epsilon_j - \lambda)/\Delta}}}{\sqrt{1 + (\epsilon_j - \lambda)/\Delta}}$ and $\alpha'_0 = \sum_j (j + 1/2) U'_j V'_j =$

$\sum_j (j + 1/2) \frac{1 - \frac{(\epsilon_j - \lambda)/\Delta}{\sqrt{1 + (\epsilon_j - \lambda)/\Delta}}}{\sqrt{1 + (\epsilon_j - \lambda)/\Delta}}$ making use as inputs ϵ_ν and N_0 , that is single-particle energies and the average number of particles.

Similar arguments can be used regarding the excitation of pairing vibrations in terms of Cooper pair transfer from closed shells as compared to one-particle transfer. As seen from Fig. 2.1.5 (b)–(c), the random phase approximation (RPA) amplitudes X_ν^a and Y_ν^a sum coherently over pairs of time reversal states²⁵ to give rise to the spectroscopic amplitudes associated with the direct excitation of the pair addition mode displayed in (d). Because of the (dispersion) relation (b)+(c) \equiv (d), the X_ν - and Y_ν -amplitudes are correlated, among themselves as well as in phase. As seen from (g) and (h), the situation is quite different in the case of one-particle transfer. The soundness of the above parlance reflects itself in the calculation of the elements resulting from the encounter of structure and reaction, namely one- and two-nucleon modified transfer formfactors. While it is usually considered that these quantities carry all the structure information associated with the calculation of the corresponding cross sections, a consistent NFT treatment of structure and reaction will posit that equally much is contained in the distorted waves describing the relative motion of the colliding systems. This is because the state dependent components of the optical potential which determines the scattering waves, emerges from the same elements, eventually including also inelastic transition densities, used in the calculation of the structure properties²⁵. In other words, to describe a

²³ See Sect. 2.4.2, see Potel, G. et al. (2013b).

²⁴ Brink, D. and Broglia (2005) Ch. 5.

²⁵ See Sect. 3.5; cf also Broglia, R. A. et al. (1981), Pollarolo et al. (1983), Broglia and Winther (2004), Fernández-García, J.P. et al. (2010), Fernández-García, J.P., M. Rodríguez-Gallardo et al.

$$N_0 = \sum_j V_j^2 = \sum_j \left(\frac{2j+1}{2} \right) \left(\frac{1}{1 + (\epsilon_j - \lambda)^2 / \Delta^2} \right)$$

and gap equation $\frac{1}{G} = \sum_{j \neq 0} \frac{1}{2E_j} = \frac{1}{\Delta'} \sum_j \left(\frac{2j+1}{2} \right) U'_j V'_j = \frac{\alpha'_0}{\Delta'}$
i.e. $\alpha'_0 = \Delta'/G$

CH₃

| v_{np} | U_N |
|----------|-------|
| p, t | |
| (t, p) | |

Table 3.1.1

Xerox copy Ch. 3
 Sept. 193
 Ch. 3
 Version, Oct 2+,
 2017
 Also 1st p. CH3
 (III) version Sept. 18
 2017

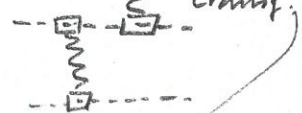
Chapter 3

Pair transfer in a nutshell

3.1 Simultaneous versus successive Cooper pair transfer in nuclei

Cooper pair transfer is commonly thought to be tantamount to simultaneous transfer. In this process a nucleon goes over through the NN -interaction v , the second one does it making use of the correlations with its partner (cf. Figs. 3.1.1 and 5.C.1 (I)). Consequently, in the independent particle limit, simultaneous transfer should not be possible (see App. 5.C.1). Nonetheless, it remains operative. This is because, in this limit, the particle transferred through v does it together with a second one which profits from the non-orthogonality of the wavefunctions describing the single-particle motion in target and projectile (Figs. 3.1.2 and 5.C.1 (II)). This is the reason why this (non-orthogonality) transfer amplitude has to be treated on equal footing with the previous one representing, within the overcomplete basis employed, a natural contribution to simultaneous transfer (cf. also the discussion carried out in Ch.2 in connection with the overlap Ω_n Eq. (2.1.3)). In other words, $T^{(1)}$ gives the wrong cross section, even at the level of simultaneous transfer, as it violates two-nucleon transfer sum rules¹. In fact $(T^{(1)} - T_{NO}^{(1)})$ is the correct, sum rule conserving two-nucleon transfer amplitude to lowest order (first) in v (Fig. 3.1.2). The resulting cancellation is quite conspicuous in actual nuclei (see e.g. Figs. 3.4.2 (b) and 3.4.3, see also Fig. 3.4.4). This is in keeping with the fact that Cooper pairs are weakly correlated systems and the reason why the successive transfer process in which v acts twice (implying the mean field U in the post-post representation²), is the dominant mechanism in pair transfer reactions (Sect. 3.3). While this mechanism seems antithetical to the transfer of correlated fermions pairs (bosons), it probes, in the nuclear case, the same pairing correlations as simultaneous transfer does (Sect. 3.4). This is because nuclear Cooper pairs (quasi-bosons) are quite extended objects, the two nucleons being (virtually)

Correlar con
 App. 5C en particular
 Fig. 5.C.2 posiblemente
 equivocada



2, like
 Sagnac current
 on 2e

¹Broglia, R. A. et al. (1972), Bayman, B. F. and Clement (1972); cf. also Sect. 1.2

²Potel, G. et al. (2013a), Eq. (A7). Within this context see also Pinkston and Satchler (1982).

(a-a) pp. (229)_a + (229)_b

3.7. PHASE COHERENCE

229

where

$$a'_v^\dagger = \mathcal{G}(\phi) a_v^\dagger G^{-1}(\phi) = e^{-i\phi} a_v^\dagger (a'_v^\dagger = e^{-i\phi} a_v^\dagger),$$

$$U_v = |U_v| = U'_v; \quad V_v = e^{-2i\phi} V'_v (V'_v = |V_v|).$$

(3,7,8)

and

$$|BCS(\phi)\rangle_{\mathcal{K}} = \left(\prod_{v>0} U_v \right) \sum_N e^{-iN\phi} \left(\sum_{v>0} c_v P_v'^\dagger \right)^{N/2} |0\rangle,$$

with

$$c_v = \frac{V_v}{U_v}; \quad P_v'^\dagger = a_v'^\dagger a_v'^\dagger,$$

is a wavepacket in particle number,

$$|BCS(\phi)\rangle_{\mathcal{K}} = \left(\prod_{v>0} U_v \right) \sum_N e^{-iN\phi} |N\rangle. \quad (3.7.1)$$

Let us now apply the gauge angle operator

$$\begin{aligned} \hat{\phi}|BCS(\phi)\rangle_{\mathcal{K}} &= i \frac{\partial}{\partial N} |BCS(\phi)\rangle_{\mathcal{K}} \\ &= \phi \left(\prod_{v>0} U_v \right) \sum_N e^{-iN\phi} |N\rangle = \phi |BCS(\phi)\rangle_{\mathcal{K}}. \end{aligned}$$

Thus the state $|BCS(\phi=0)\rangle_{\mathcal{K}}$ is rigidly aligned in gauge space in which it defines a privileged orientation (z').

An isolated nucleus will not remain long in this product type state. Due to the term $(G/4) \left(\sum_{v>0} (U_v^2 + V_v^2) (\Gamma_v^\dagger - \Gamma_v) \right)^2$ in the residual quasiparticle Hamiltonian it will fluctuate (QM, ZPF, Goldstone mode), and decay into a state

$$|N\rangle \sim \int d\phi e^{iN\phi} |BCS(\phi)\rangle_{\mathcal{K}}, \quad (3.7.2)$$

16

0,092

member of a pairing rotational band around neutron mass number N : for example the ground states of the Sn-isotopes around $N_0 = 68$ (see Fig. 2.1.3). Because $E_R = (\hbar^2/2I)(N - N_0)^2 = (G/4)(N - N_0)^2 = G/4(\frac{1}{\delta\phi})^2$ is the kinetic energy of rotation in (nuclear) gauge space, and $G/4 \approx 25/(4N_0) \approx 0.0092$ MeV, the wavepacket (3.7.1) will decay⁴⁵ in the state (3.7.2) in a time of the order of $\hbar/E_R \approx$

⁴⁵Within this context note that setting in phase at $t = 0$ all the states in which a GDR breaks down through the hierarchy of doorway-states-coupling, they would dissipate like a wavepacket of free particles after 10^{-22} sec (assuming $\Gamma_{GDR} \approx 3 - 4$ MeV). It is of notice that the GDR will eventually branch into the ground state, although $\Gamma_y \ll \Gamma_{GDR}$, in keeping with the fact that the $t = 0$ phase coherent states are, individually, stationary. What is not stationary is its phase coherence (see Sect. 1.3). Pushing the analogy a step further, one can say that in quantum mechanics, while the outcome of an experiment is probabilistic the associated probability evolve in a deterministic way (Born (1926)). This is the reason why a large gamma ray detector will reveal a well defined peak of the resonant dipole state long after its lifetime deadline (\hbar/Γ). Also, one can obtain a completely (classical) picture of a face making use of single photons at a time, provided one waits long enough.

*) See Brink and Broglia (2005) Sect. 4.2.2 and for more details APPS, H, I and J.

**) In these estimates the approximate value $\hbar/1\text{MeV} \approx (2/3) \times 10^{-21}\text{s}$ is used

ref. find
- where in
the book
we talk

see end Caption Fig. 2.1.2

p. 131

p. (229) C hand-
written and
attached to
this page

(a) One can rewrite (3.7.7) as

(229)
a

$$\begin{aligned} |\text{BCS}(\phi)\rangle_K &= \prod_{v>0} (U'_v + e^{-2i\phi} V'_v a_v^\dagger a_v^\dagger) |0\rangle \\ &= \left(\prod_{v>0} U'_v \right) \prod_{v>0} (1 + e^{-2i\phi} C_v P_v^\dagger) |0\rangle \quad (3.7.9) \end{aligned}$$

where

$$C_v = \frac{V'_v}{U'_v} \quad (3.7.10)$$

Working out the above relation making use of the fact that $(P_v^\dagger)^2 = 0$ and $P_v^\dagger P_{v1}^\dagger = P_v^\dagger P_{v1}^\dagger$, as we are dealing with fermions one obtains,

$$|\text{BCS}(\phi)\rangle_K = \left(\prod_{v>0} U'_v \right) \sum_n \frac{1}{n!} \left(\sum_{v>0} e^{-2i\phi} C_v^\dagger P_v^\dagger \right)^n |0\rangle, \quad (3.7.11)$$

where $n = 0, 1, 2, \dots$ is the number of pairs, i.e.

$$n = \frac{N}{2}. \quad (3.7.12)$$

that is, a wavepacket in particle number.

Thus

$$|\text{BCS}(\phi)\rangle_K = \left(\prod_{v>0} U'_v \right) \exp \left(\sum_{v>0} C_v^\dagger e^{-2i\phi} P_v^\dagger \right), \quad (3.7.13)$$

which testifies to the fact that the BCS-ground is a coherent state defining a privileged orientation in phase space.

In fact, making use of (3.7.12) one can write (3.7.14) as

$$|\text{BCS}(\phi)\rangle_K = \left(\prod_{v>0} U'_v \right) \sum_{N \text{ even}} \frac{1}{(N/2)!} e^{-iN\phi} \left(\sum_{v>0} C_v^\dagger P_v^\dagger \right)^{\frac{N}{2}} |0\rangle. \quad (3.7.14)$$

Thus

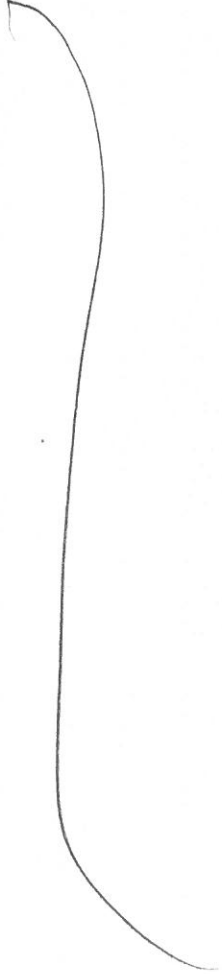
$$\hat{\phi} |\text{BCS}(\phi)\rangle_K = -i \frac{\partial}{\partial N} |\text{BCS}(\phi)\rangle_K = \phi |\text{BCS}(\phi)\rangle_K.$$

(a) (3.7.15)

App. A of

*) Following Brink and Broglia (2005) one can write $[P_v^+, P_{v1}^+] = a_v^+ [a_v^+, P_v^+] + [a_v^+, P_{v1}^+] a_v^+$
Because $[a_v^+, P_v^+] = -[a_{v1}^+, \{a_v^+, a_{v1}^+\}] + \{a_v^+, a_{v1}^+\} a_v^+ = 0$
 and similar for $[a_v^+, P_{v1}^+]$ implies $[P_v^+, P_{v1}^+] = 0$.
 This technical detail testifies to the fact that Cooper pair condensation as embodied in the coherent state (3, 7, 13) is rather different, although displaying important similarities, with Bose-Einstein condensation.

— italics.



* Within BCS theory of pairing, there are two parameters which determine spontaneous symmetry breaking in gauge space. The probability amplitudes with which a pair state ($\nu\bar{\nu}$) is occupied, and that with which it is empty. Namely V_ν and U_ν respectively. As a consequence, there are only two fields F which contribute, through terms of type FF^+ , to the residual interaction H_{res} acting among quasiparticles, which is neglected in the mean field solution of the pairing Hamiltonian. One which is antisymmetric with respect to the Fermi energy, namely $(U_\nu^2 - V_\nu^2)$ and leads to pairing vibrations of the gauge deformed state $|BCS\rangle$. The other one, $U_\nu^2 + V_\nu^2$, is symmetric with respect to E_F and leads to fluctuations which diverge in the long wavelength limit ($W_i'' \rightarrow 0$) in precisely the right way to set $|BCS\rangle$ into rotation with a finite inertia, and restore symmetry. This term is written as

$$\begin{aligned} H''_p &= \frac{G}{4} \left(\sum_{\nu \neq 0} (U_\nu^2 + V_\nu^2) (\Gamma_\nu^+ - \Gamma_\nu^-) \right)^2 \\ &= \frac{G}{4} \left(\sum_{\nu \neq 0} (\Gamma_\nu^+ - \Gamma_\nu^-) \right)^2 \end{aligned}$$

where Γ_ν^+ (Γ_ν^-) is the two quasiparticle creation (annihilation) operator in the harmonic (quasiboson) approximation: $[\Gamma_\nu, \Gamma_\nu^\pm] = \delta(\nu, \nu)$.

~~Brink and Broglie (2005) Eq(4,24) and Sect. I.4, for more detail see App.3 of this reference.~~

$\hbar/(\hbar^2/2\pi) \approx \hbar/(0.092 \text{ MeV}) \approx 10^{-20} \text{ s}$, more accurately, because^{*} $N = N_0 \pm 2$, $\hbar/E_R \approx \hbar/(4 \times 0.092 \text{ MeV}) \approx 2 \times 10^{-21} \text{ s}$.

230 CHAPTER 3. SIMULTANEOUS VERSUS SUCCESSIVE TRANSFER

9.5

$\hbar/(4 \times 0.092 \text{ MeV}) (N = N_0 \pm 2) \approx 10^{-19} \text{ sec}$. In other words, superfluid nuclei cannot be prepared, in isolation, in states with coherent superposition of different N -values. The common assumption that N is fixed, ϕ meaningless is correct. This is also the case for real superconductors. In fact, the corresponding state (3.7.1) even if prepared in isolation would dissipate because there is actually a term in the energy of the superconductor depending on N , namely the electrostatic energy $e(N - N_0)^2/2C = e^2/2C(\partial/\partial\phi)^2$, where C is the electrostatic capacity. The system will dissipate, no matter how small $\delta\phi$ is. In fact, let us assume $\delta\phi = 1$ degree ($= \pi/180 = 0.017$). The kinetic energy of rotation in gauge space is of the order of $(e^2/2C)(1/\delta\phi)^2$ (of notice that $\delta N \delta\phi/2\pi \rightarrow 1$), and

$$\Delta E = \frac{1.44 \text{ fm MeV}}{1 \text{ cm } (1^\circ)^2} \sim 1.44 \times 10^{-13} \text{ MeV}, \quad (3.7.3)$$

which corresponds to an interval of time

$$\Delta t \approx \frac{\hbar}{1 \text{ MeV}} \frac{10^{13}}{1.44} \approx \frac{0.667 \times 10^{-21} \text{ sec}}{1.44} \times 10^{13} \approx 10^{-9} \text{ sec}. \quad (3.7.4)$$

already
checked with
P.W. Anderson
Cianciello

The opposite situation is that of the case in which one considers different parts of the same superconductor. In this case one can define relative variables $n = N_1 - N_2$ and $\phi = \phi_1 - \phi_2$ and again $n = -i\partial/\partial\phi$ and $\phi = i\partial/\partial n$. Thus, locally there is a superposition of different n states: ϕ is fixed so n is uncertain. It is clear that there must be a dividing line between these two behaviors, perfect phase coherence and negligible coherence, namely the Josephson effect.

In the nuclear case, one can view the systems $|BCS(A+2)\rangle$ and $|BCS(A)\rangle$ as parts of a fermion superfluid (superconductor) which, in presence of a proton ($p + (A+2)$) are in weak contact to each other, the $d + |BCS(A+1)\rangle$ system (without scattering, running waves, but as a closed, virtual, channel) acting as the dioxide layer of a Josephson junction (Fig. 3.7.1).

Clearly, again, the total phase of the assembly is not physical. However, the relative phases can be given a meaning when one observes, as one does in e.g. metallic superconductors, that electrons can pass back and forth through the barrier, leading to the possibility of coherence between states in which the total number of electrons is not fixed *locally*. Under such conditions there is, for instance, a coherence between the state with $N/2$ electrons in one half of the block and $N/2$ in the other, and that with $(N/2) + 2$ on one side and $(N/2) - 2$ on the other.

Under favorable conditions, in particular of Q -value for the different channels involved and, similarly to the so called backwards rise effect, one may, arguably, observe signals of the coherence between systems $(A+2)$ and A in the elastic scattering process ${}^{A+2}X + p \rightarrow {}^A X + t$ (t denoting a member of a pairing rotational band (cf. Fig. 3.7.1, see also Fig 2.1.3)). Fig. 3.7.1

Whether an effect which may parallel that shown in (c) (backwards rise) can be seen or not depends on a number of factors, but very likely it is expected to be a weak effect. This was also true in the case of the Josephson effect in its varied versions (AC, DC, etc.). In fact, its observation required to take into account the effect of the earth magnetic field, let alone quantal and thermal fluctuations.

① - ②
pp.
(230)
(230)

- *1) Implying $\Delta\phi \approx 1/\Delta N = 0.5 \approx \frac{0.5}{(\pi/180^\circ)} \approx 30^\circ$, a rather large number, in keeping with the small number (5-6) of Cooper pairs participating in the nuclear condensate.

Ksh. 17/12/17

C) (b) - (b) (see lower part this page and ~~(230)~~)
 In the case of a single j-shelf ~~**~~ model*, to rewrite
 (3.7.10), ~~that is~~. In this model,
 $V' = \sqrt{\frac{N}{2\pi^2}}, V' = \sqrt{1 - \frac{N}{2\pi^2}}.$ ~~(3.7.15)~~ (3.7.17)

Thus

$$U'V' = \sqrt{\frac{N}{2\pi^2} \left(1 - \frac{N}{2\pi^2}\right)} \quad \cancel{(3.7.17)} \quad (3.7.18)$$

while

$$\frac{V'}{U'} = \sqrt{\frac{N}{2\pi^2 - N}}. \quad (3.7.19)$$

For a number of particles considerably smaller than the full degeneracy of the single-particle subspace in which nucleons can correlate, i.e. for $N \ll 2\pi^2$, one can write

$$U'V' = \sqrt{\frac{N}{2\pi^2}} \left(1 - \frac{N}{4\pi^2}\right) \approx \sqrt{\frac{N}{2\pi^2}}, \quad (3.7.20)$$

and $\frac{V'}{U'} \approx \sqrt{\frac{N}{2\pi^2}} \left(1 + \frac{N}{4\pi^2}\right) \approx \sqrt{\frac{N}{2\pi^2}} \approx U'V'$ ~~(3.7.21)~~

Consequently, the Cooper pair wavefunction can be written as

$$\sum_{v>0} e^{-2i\phi} \frac{V'_v}{U'_v} a_v^\dagger a_v^\dagger \approx \sum_{v>0} U'_v V'_v a_v^\dagger a_v^\dagger \quad (3.7.22)$$

b) Let us conclude this section^b
 As already stated, the members of the pairing rotational band are ('see Eq. ~~(3.7.14)~~ (3.7.15)) ~~(3.7.15)~~ (3.7.15)

$$|N_0\rangle = \int d\phi e^{iN_0\phi} |BCS(\phi)\rangle_K \sim \left(\sum_{v>0} c_v^\dagger a_v^\dagger a_v^\dagger \right)^{N_0/2}$$

From this relation it emerge, that the Cooper pair wavefunction,

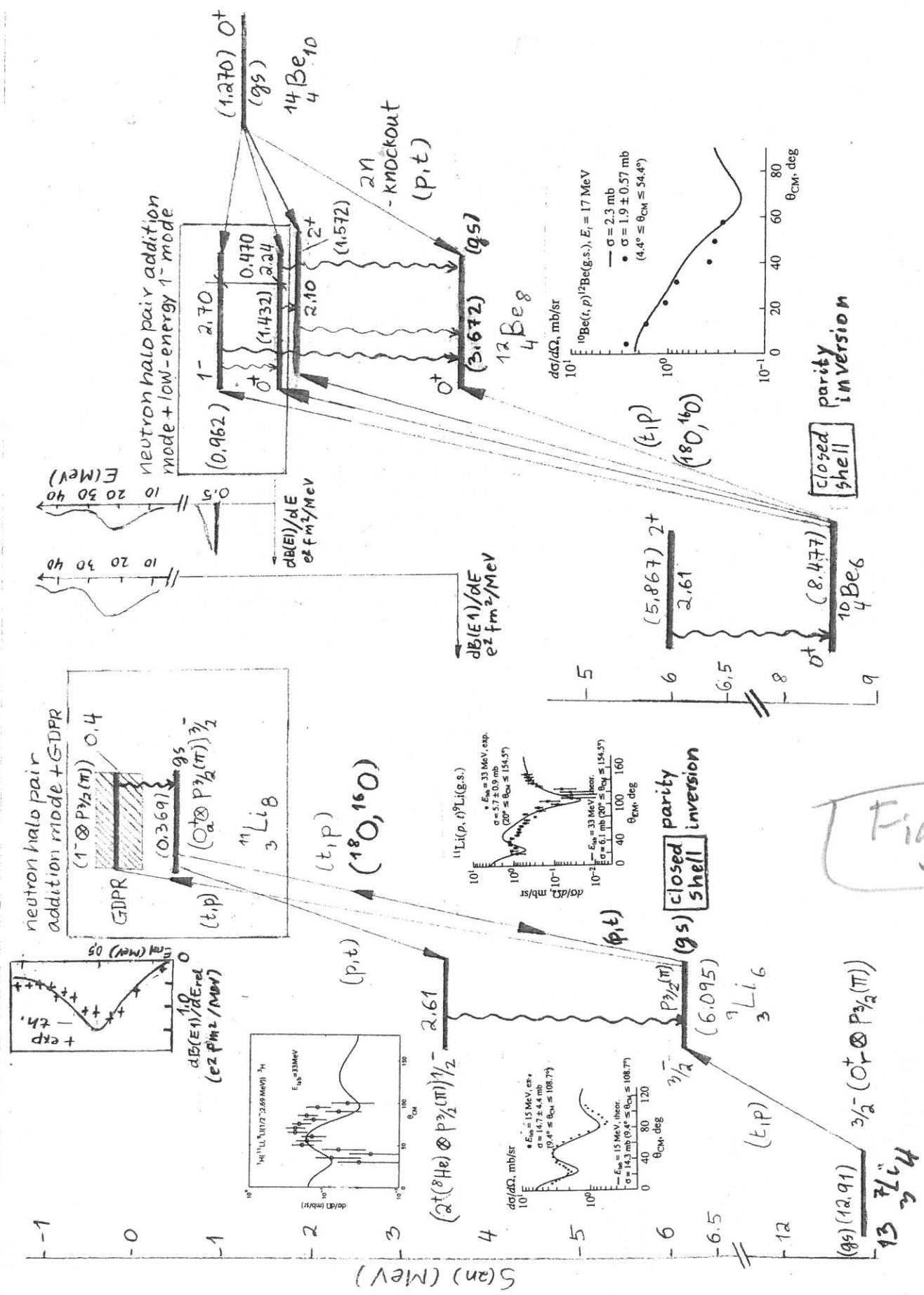
$$|\tilde{10}\rangle = \sum_{v>0} c_v a_v^\dagger a_v^\dagger |10\rangle, \quad (3.7.16)$$

^{a)} See e.g. Brink and Broglie (2005) App. H

^{**} See e.g. Potel et al (2013), Eq. (B15)

Kofb 17/12/17
is to be interpreted to be valid for values (230)
of ϵ_v close to ϵ_F . This is because BCS superfluidity
affects only the occupation numbers U'_v, V'_v within a
narrow band ~~and around~~ around ~~the~~ around
around the Fermi energy ($\epsilon_F \pm \Delta$). Within
this context, one can ~~not~~ make use of the (b) ~~for~~

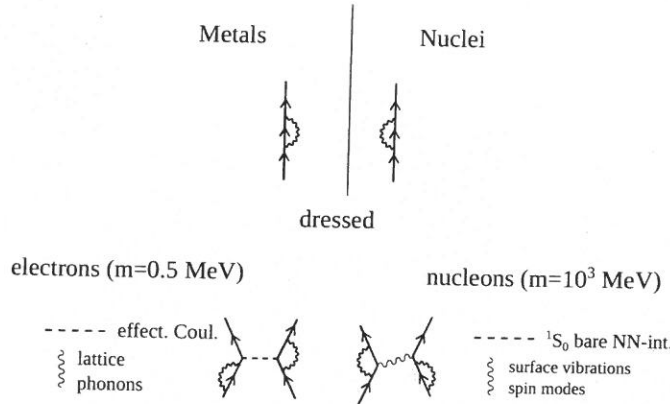
1.1.2017



$$\begin{aligned}
t_{FC} &= 2 \times 10^3 \text{ eV} \text{ Å} = 2 \times 10^6 \text{ meV} \text{ Å} ; m_F c^2 = 0.5 \times 10^6 \text{ eV} ; \frac{(t_{FC})^2}{2m_F c^2} = 4 \times 10^{-8} \text{ eV} = 4 \times 10^{-5} \text{ meV} \\
C &= 3 \times 10^{10} \text{ cm/s} ; V_F = 1.83 \times 10^8 \text{ cm/sec (Pb)} ; V_F = 2.03 \times 10^8 \text{ cm/sec (Al)} \\
(V_F/c) &= \begin{cases} 0.61 \times 10^{-2} (\text{Pb}) \\ 0.68 \times 10^{-2} (\text{Al}) \end{cases} \quad \Delta = \begin{cases} 1.4 \text{ meV (Pb)} \\ 0.18 \text{ meV (Al)} \end{cases} ; \xi = \frac{\hbar V_F}{\pi \Delta} = \left(\frac{\hbar c}{\pi} \right) \times \left(\frac{V_F/c}{\Delta} \right) = 0.64 \times 10^6 \text{ meV} \text{ Å} \times \begin{cases} 0.43 \times 10^2 \text{ meV}^{-1} \\ 3.78 \times 10^2 \text{ meV}^{-1} \end{cases} \\
\frac{(t_{FC})^2}{2m_F} &= 4 \text{ eV} \text{ Å} = 4 \times 10^3 \text{ meV} \text{ Å}^2 \quad q_\xi = \frac{\hbar^2}{2m_F \xi^2} \frac{1}{2\Delta} \approx \begin{cases} 1.6 \times 10^{-4} (\text{Pb}) \\ 1.9 \times 10^{-5} (\text{Al}) \end{cases} = \begin{cases} 0.13 \times 10^4 \text{ Å} (\text{Pb}) \\ 2.14 \times 10^4 \text{ Å} (\text{Al}) \end{cases}
\end{aligned}$$

3.B. COOPER PAIR: RADIAL DEPENDENCE

251



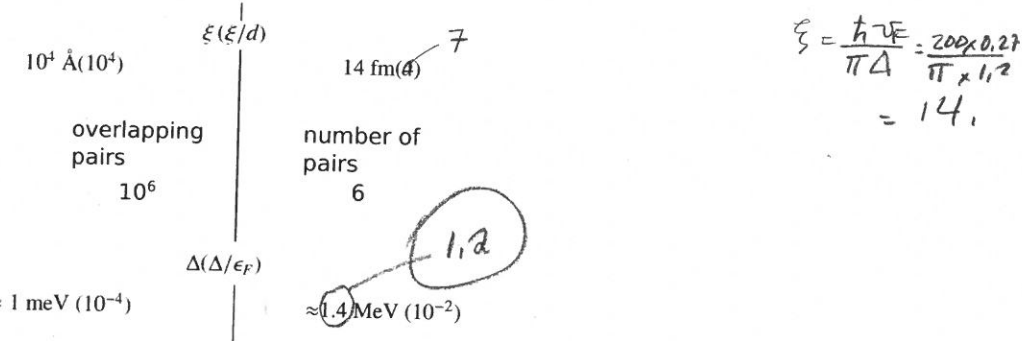
Corrected

16/12/2017

spontaneous breaking of gauge symmetry

$$(U'_v + V'_v e^{-2i\phi} a_v^\dagger a_v^\dagger) |0\rangle \quad \checkmark$$

independent pair motion



$$\xi = \frac{\hbar \tau E}{\pi \Delta} = \frac{200 \times 0.27}{\pi \times 14^2} = 14,$$

generalized quantity

parameter

$$q_\xi = \frac{\hbar^2}{2m_\xi^2} \frac{1}{2\Delta} = 0.04$$

$$\frac{\hbar^2}{2m(14)^2} \frac{1}{2 \cdot 4}$$

$$\approx \frac{240}{(14)^2 \cdot 2 \cdot 4}$$

$$\approx 0.085$$

$$\approx 0.1$$

check
done
27/12/17

$P_1 = 10^{-10}$
observation of supercurrents of 2e carriers (Josephson effect) between two weakly coupled superconductors separated by a barrier allowing essentially for single electron tunneling

Single Cooper pair tunneling between members of a pairing rotational band satisfying

$$\frac{\sigma(gs(N) \rightarrow gs(N+2))}{\sum_{exc} \sigma(gs(N) \rightarrow 0_{exc}^+(N+2))} \gg 1$$

thus fulfilling

$$P_2 \approx P_1$$

$$(\sigma_1 \approx \sigma_2)$$

Figure 3.A.5

Probing gauge deformation with one-electron tunneling / -nucleon transfer probability

$$P_1 = 10^{-10}$$

$$P_1 = 10^{-3}$$

one observes

vibrations

(ph) | (pp) (hh)

correlated excitations (E_{corr})
with transfer quantum numbers

$\beta=0$ | $\beta=\pm 2$

waves on

the nuclear | the Fermi
surface

correlation length

$$\xi \approx \frac{\hbar v_F}{\pi E_{\text{corr}}}$$

typical values $E_{\text{corr}} = -2 \text{ MeV} (-0.5 \text{ MeV}, \text{halo})$; $k_F = 1.36 \text{ fm}^{-1}$, $v_F \approx 37 \text{ MeV}$, $v_F/c = 0.27$ (0.8 fm^{-1} , 13 MeV , 0.16)

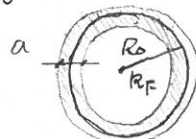
$$\xi \approx 14 \text{ fm} (20 \text{ fm}, \text{halo})$$

generalized quantity parameter

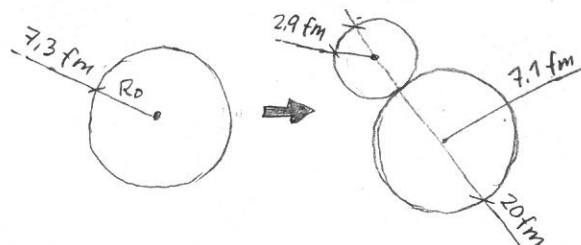
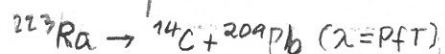
$$q_\xi = \frac{\hbar^2}{2m(\xi)^2} \frac{1}{|E_{\text{corr}}|} \approx 0.05 (0.1 \text{ halo})$$

strongly correlated ($q_\xi \ll 1$), weakly "bound" ($|E_{\text{corr}}|/v_F \approx 0.5$ (0.4 halo))
extended objects $\xi/d \gtrsim 7$ ($d = (\frac{4\pi R^3}{3A})^{1/3}$)

subject to a strong external field



example



$$\langle r^2 \rangle_{\text{def}}^{1/2} = \xi = \frac{\hbar v_F}{\pi |E_{\text{corr}}|} \approx 29 \text{ fm}$$

$(E_{\text{corr}} \approx 0.6 \text{ MeV})$

$$\langle r^2 \rangle_{\text{cooper}}^{1/2} = \xi = \frac{\hbar v_F}{\pi \Delta} \approx 21 \text{ fm}$$

$(\Delta \approx 0.8 \text{ MeV})$

Fig. 3.3.3

$$E_F \frac{\hbar^2 k_F^2}{2m} = 20 \text{ MeV fm}^2 \times \begin{cases} (1.36)^2 \text{ fm}^2 \\ (0.8)^2 \text{ fm}^2 \end{cases} \approx \begin{cases} 37 \text{ MeV} \\ 13 \text{ MeV} \end{cases}$$

$$\frac{2 \text{ MeV}}{37 \text{ MeV}} \approx 0.05 \quad \frac{0.5 \text{ MeV}}{13 \text{ MeV}} \approx 0.04$$

3.B. COOPER PAIR: RADIAL DEPENDENCE

259

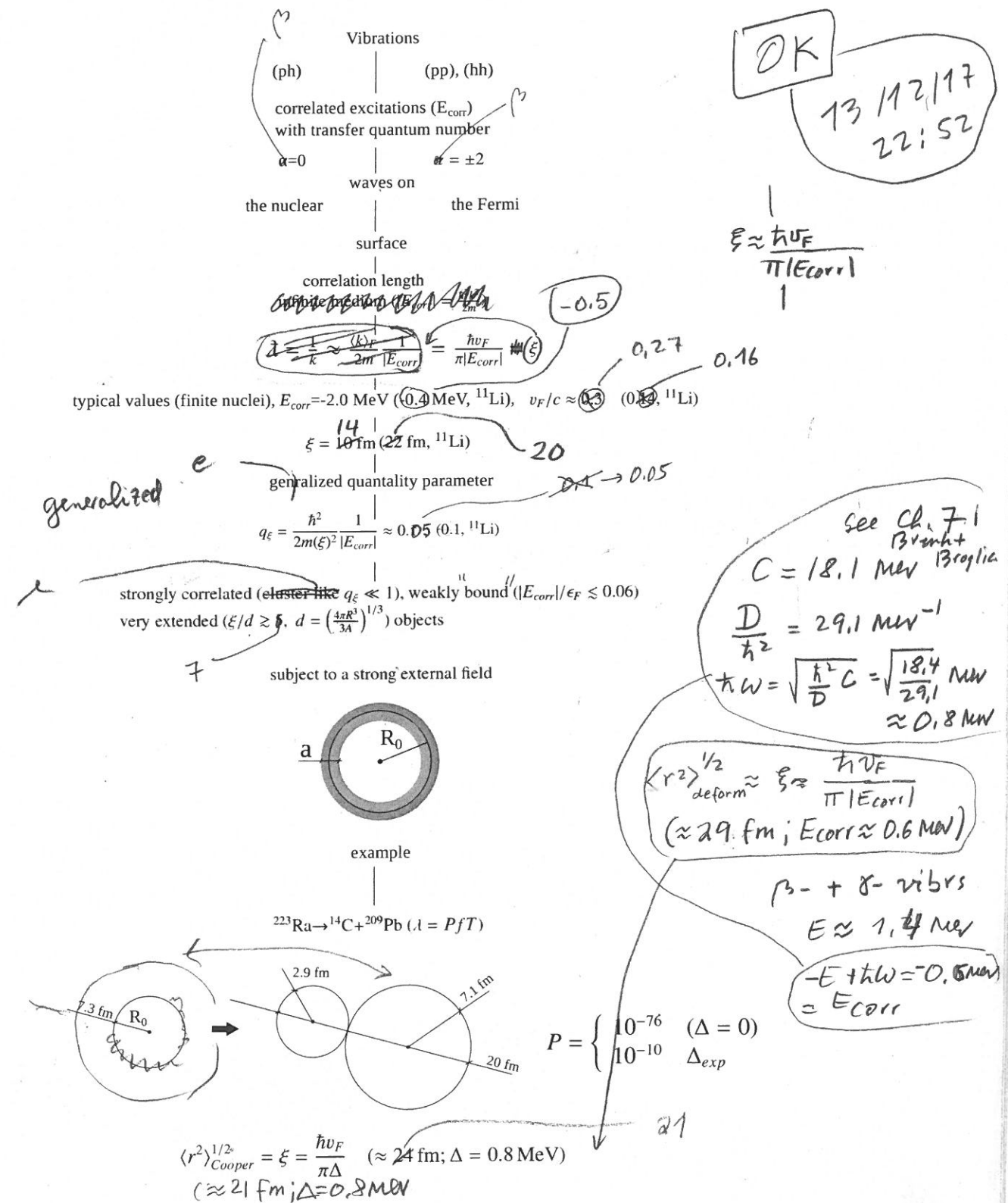


Figure 3.B.3

CH₄

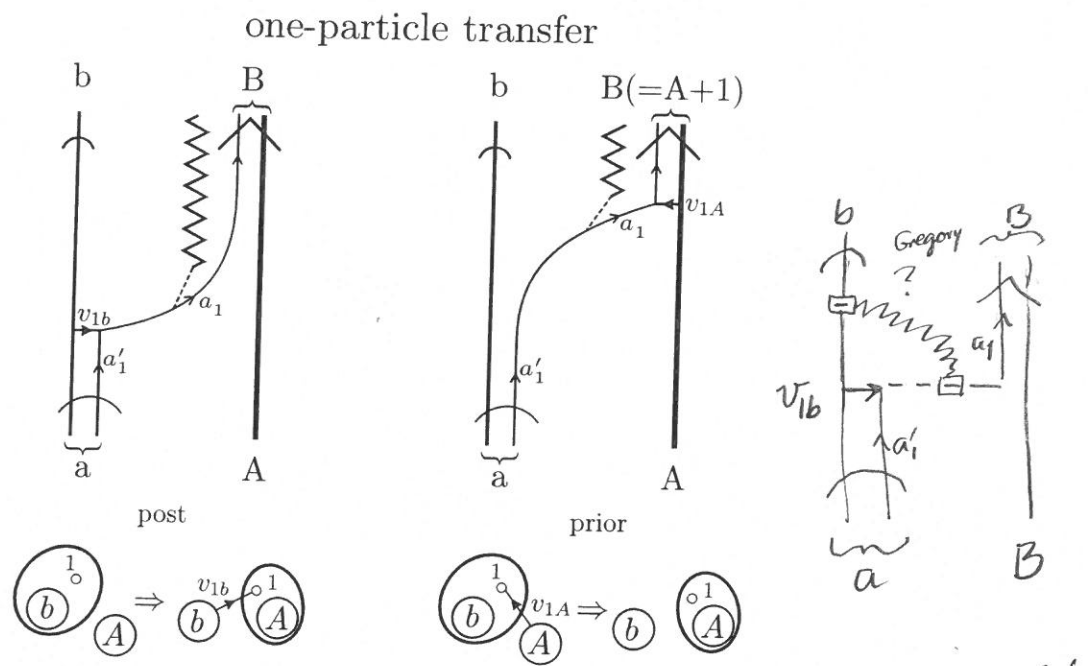
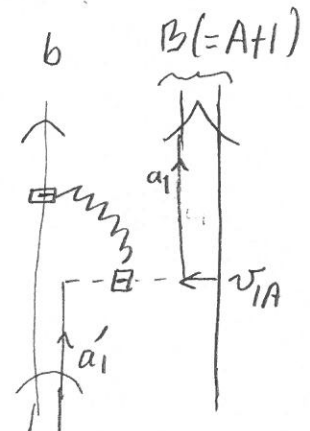


Figure 4.1.1: NFT graphical representation of the one-particle transfer reaction $a = b + 1 + A \rightarrow b + B (= A + 1)$ (for details in the notation we refer to Figs. 5.C.1 and 5.C.2 and to the last paragraph before Sect. 5.C.1 of App. 5.C). The time arrow is assumed to point upwards. The quantum numbers characterizing the states in which the transferred nucleon moves in projectile and target are denoted a'_1 and a_1 respectively. The interaction inducing the nucleon to be transferred can act either in the entrance channel $((a, A); v_{1A}$, prior representation) or in the exit channel $((b, B); v_{1b}$, post representation), in keeping with energy conservation. In the transfer process, the nucleon changes orbital at the same time that a change in the mass partition takes place. The corresponding relative motion mismatch is known as the recoil process, and is represented by a jagged curve (this is the recoil elementary mode, mode which couples to the particle degrees of freedom through a Galilean transformation operator). The recoil mode provides information on the evolution of r_{1A} (r_{1b}). In other words, on the coupling between structure and reaction (relative motion) degrees of freedom.

mean field?



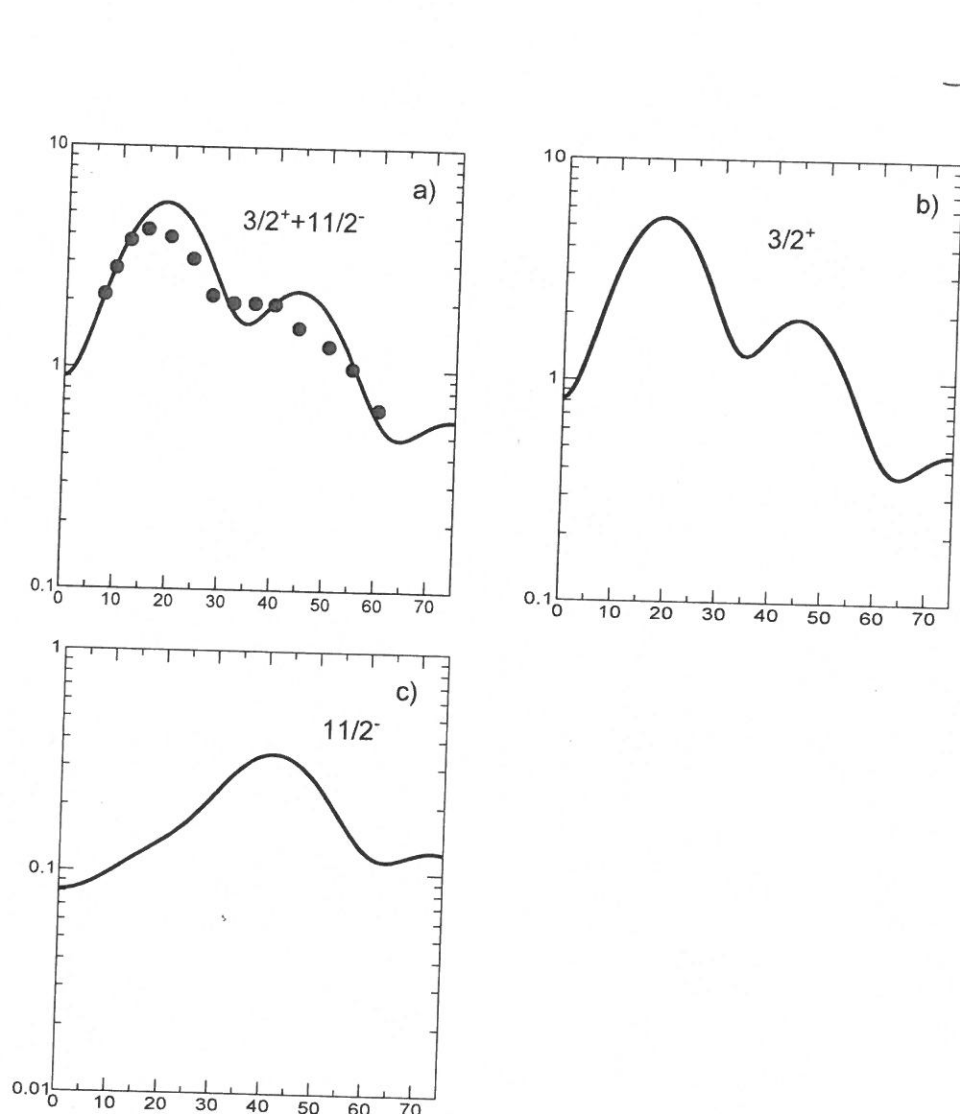


Figure 4.2.2: The theoretical absolute differential cross section (continuous curve) associated with the reaction $^{120}\text{Sn}(d, p)^{121}\text{Sn}$ and populating the low-lying states $3/2^+$ and $11/2^-$ are shown in b) and c), while the summed differential cross section is displayed in a) in comparison with the data (Bechara, M. J. and Dietzsch (1975)).

FRESCO

Comparison

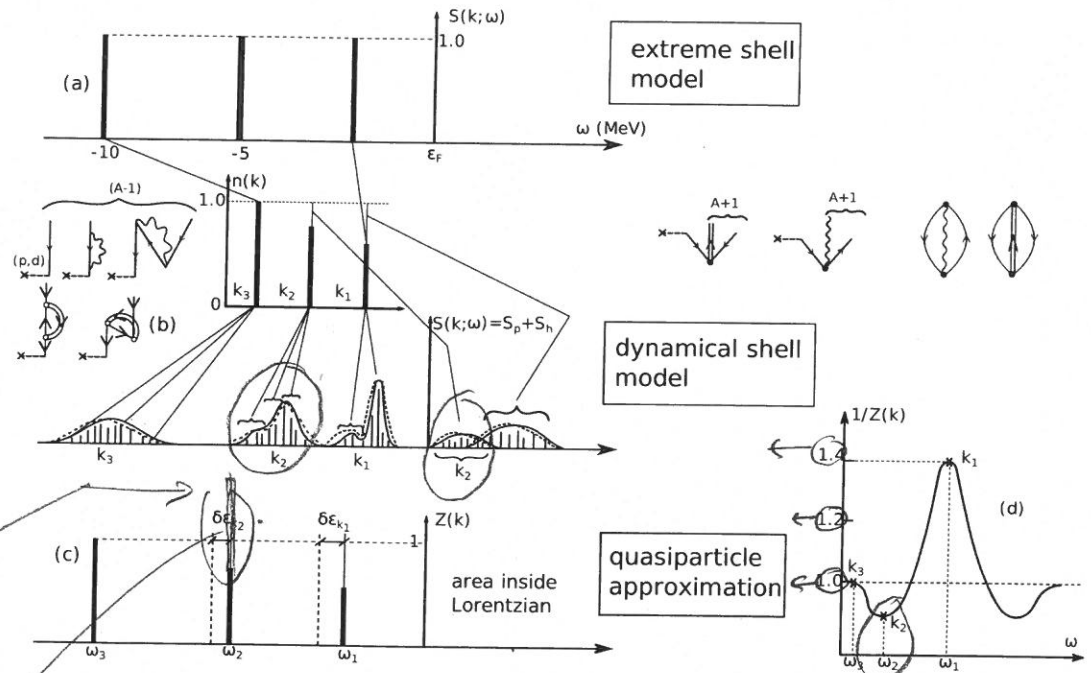
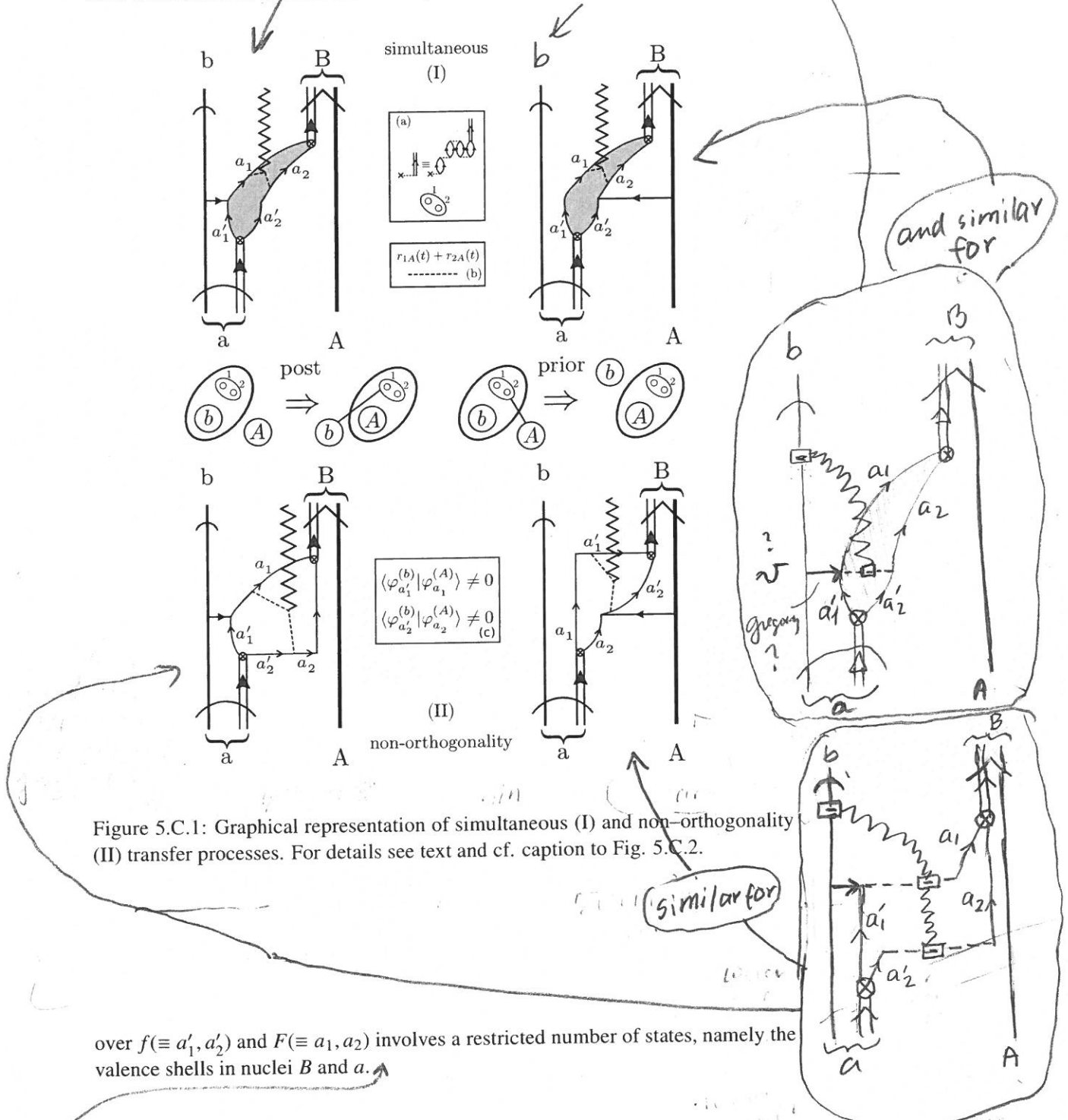


Figure 4.H.1: Schematic representation of the main quantities characterizing the single-particle motion in the nuclear shell model taking into account the residual interaction among the particles at different levels of approximation. In (a) the interaction is treated in the Hartree-Fock approximation and the particles feel the presence of the other particles through their own confinement in the average field. The strength function shows sharp peaks, each of them carrying the full strength of the states. In fact, the occupation number associated with each state k contains only one contribution. In (b) the particles still couple only with the average field. However in this case they can set the surface into vibrations by changing its state of motion. The strength associated with each orbital is distributed over a finite energy range. The corresponding occupation numbers arise from the sum of many contributions. Fitting a Lorentzian shape to each peak one can regain the simplicity of the extreme shell model by defining new levels with energy equal to that of the centroid and strength equal to that of the area covered by the Lorentzian shape (cf. (c)). In (d) the energy variation of the shift of the centroids is contained into an effective ω -mass according to the standard relation $\frac{m_\omega}{m} = \left(1 - \frac{\partial \Delta E}{\partial \hbar \omega}\right)$ (see Eq. (4.A.5)). The resulting curve resembles the shape obtained by calculating the inverse of the area below the different Lorentzians (quasiparticle approximation).

CHS



The successive transfer amplitude $\tilde{a}_\infty^{(2)}$ written making use of the post-prior representation is equal to (see Fig. 5.C.2 (III))

It is of notice that the NFT (rt+) diagrams appearing in Fig. 5.C.1 (II) are the only ones we have encountered in which to a particle-recoil coupling vertex (dashed open rectangle) and thus the starting or/and ending of a recoil mode (jaggy line) does not correspond the action of the nuclear interaction or mean field (horizontal short arrow) inducing a transfer process.

